

1 Article

2 Nanoparticle behaviour in an urban street canyon at 3 different heights and implications on indoor 4 respiratory doses

5 Maurizio Manigrasso ^{1,*}, Carmela Protano ², Matteo Vitali ² and Pasquale Avino ³

6 Department of Technological Innovations, INAIL, Rome, Italy; m.manigrasso@inail.it

7 ² Department of Public Health and Infectious Diseases, Sapienza University of Rome, Rome, Italy;

8 carmela.protano@uniroma1.it; matteo.vitali@uniroma1.it

9 ³ Department of Agricultural, Environmental and Food Sciences (DiAAA), University of Molise,

10 Campobasso, Italy; avino@unimol.it

11 * Correspondence: m.manigrasso@inail.it

12

13 **Abstract:** The amount of outdoor particles that indoor environments receive depends on the particle
14 infiltration factors (F_{in}), peculiar of each environment, and on the outdoor aerosol concentrations
15 and size distributions. The respiratory doses received, while residing indoor, will change
16 accordingly. This study aims to ascertain to what extent such doses are affected by the vertical
17 distance from the traffic sources. Particle number size distributions have been simultaneously
18 measured at street level and at about 20 m height in a street canyon in downtown Rome. The same
19 F_{in} have been adopted to estimate indoor aerosol concentrations, due to the infiltration of outdoor
20 particles and then the relevant daily respiratory doses. Aerosol concentrations at ground floor were
21 more than double than at 20 m height and richer in ultrafine particles. Thus, although aerosol
22 infiltration efficiency was on average higher at 20 m height than at ground floor, particles more
23 abundantly infiltrated at ground level. On a daily basis, this involved a 2.5-fold higher dose at
24 ground level than at 20 m height. At both levels, such doses were greater than those estimated over
25 the period of activity of some indoor aerosol sources, therefore they represent an important
26 contribution to the total daily dose.

27 **Keywords:** Ultrafine particles; aerosol; urban street canyon; outdoor pollution; indoor air quality;
28 respiratory doses; MPPD

29

30 1. Introduction

31 Outdoor and indoor air quality is a major determinant for human health. Indeed, World Health
32 Organization estimated that air pollution kills seven million people worldwide every year and nine
33 out ten individuals are exposed to high concentrations of airborne pollutants [1]. Particulate matter
34 (PM) is one of the most relevant air pollutants, linked to the pathogenesis of several human diseases
35 involving numerous systems and apparatuses. In particular, many studies highlighted that some
36 specific PM fractions (particles diameter $\leq 10 \mu\text{m}$ and $\leq 2.5 \mu\text{m}$, defined respectively as PM₁₀ and
37 PM_{2.5}) were associated to cardiovascular, respiratory and neurodegenerative diseases [2-4]. In
38 addition, in 2015 PM in outdoor air was classified as group 1 carcinogen to humans by the
39 International Agency for Research on Cancer (IARC) [5]. Over the last years the researches focused
40 the attention on smaller particles, specifically on ultrafine particles (UFPs, that is particles with sizes
41 $\leq 100 \text{ nm}$); indeed, particles $> 2.5 \mu\text{m}$ are removed quickly (few hours) from the atmosphere due to
42 dry and wet deposition, while particles $< 1 \mu\text{m}$ persist for longer times and easily contaminate both
43 outdoor and indoor air [6-8] and/or are transported over long ranges. Besides, UFPs have high
44 number concentration, very high surface area and surface area reactivity, and small size compared
45 to the dimensions of cellular structures. These characteristics allow them a great ability of both absorb

46 of organic molecules and penetrate into cellular targets [9,10]. Recent studies reported that UFPs are
47 more toxic in comparison with larger particles and induce adverse effects on respiratory and
48 cardiovascular systems via intracellular oxidative stress activation and inflammation response [11].
49 Besides, UFPs can pass directly in brain tissue through olfactory bulb and increase the risk of
50 developing neurodegenerative diseases, in particular Alzheimer's disease [12]. Also, adverse
51 outcomes on children's health associated with UFPs exposure have been recently reported, especially
52 among children with respiratory diseases [13]. Such adverse effects on human health are of particular
53 concern, considering that UFPs are released in high concentrations from many anthropogenic sources
54 both outdoor and in many occupational and domestic scenarios [14]. Vehicular traffic is the main
55 source of UFPs in urban area [15-18]. In indoor settings, UFPs are released by devices and appliances
56 commonly used (conventional and electronic cigarettes, electric appliances, etc) or activities usually
57 practiced (cooking) [19-24]. In the last years more attention was given to indoor air quality, because
58 great part of general population spends most of the time (> 90%) in enclosed environments [25] and
59 indoor air may be of worse quality than outdoor, since indoor air pollutants are the sum of those
60 penetrated from outdoor and those directly produced indoor [26,27]. On this point, several studies
61 [28-30] have addressed the issue of vertical profiles of particle concentrations in urban areas and have
62 highlighted their relevance in terms of indoor air quality. However, to date, studies describing how
63 the different vertical aerosol concentrations and size distributions affect the aerosol doses received
64 by the respiratory system of individuals residing in the same building but at different heights are
65 lacking. Thus, the aim of the present study was to ascertain to what extent such doses are affected by
66 the vertical distance from the street level.
67

68 2. Experiments

69 2.1. Aerosol measurements

70 Atmospheric particle number-size distributions were simultaneously measured by means of two
71 TSI Fast Mobility Particle Sizer (model 3091, FMPS, Shoreview, MN, USA) located at the ground level
72 and at 20 m height in a building in downtown Rome during winter season. The site (41°53'46''N,
73 12°29'46'E) was characterized by high density of vehicular traffic, it was in a narrow double lane
74 street (street width, W , of about 8 m), with high buildings on both sides (average height, H , of about
75 25 m). Such street can be considered a street canyon, as the aspect ratio H/W is about 3:1. FMPS counts
76 and classifies particles, according to their electrical mobility, in 32 size channels, in the range 5.6-560
77 nm, with 1 s time resolution. It operates at a high flow rate (10 L min⁻¹) to minimize diffusion losses
78 of UFPs and at ambient pressure, to prevent evaporation of volatile and semi-volatile particles [31].
79 The performance of the FMPS was investigated by Jeong et al. [32] by comparison with a Scanning
80 Mobility Particle Sizer (SMPS). The authors evaluated that the SMPS number concentration, in the
81 size range from 6 nm to 100 nm, is about 34% lower than the FMPS measurements, due to the
82 diffusion losses of particles in the SMPS. The diffusion loss corrected SMPS number concentration is
83 on average about 15% higher than the FMPS data. One-day outdoor aerosol measurements were
84 selected to calculate the indoor aerosol concentration inside the building at the ground floor and at
85 the 5th floor (20 m height) utilizing the size-resolved average infiltration factors (F_{in}) measured by
86 Bennett and Koutrakis [33], using time-dependent aerosol concentrations (0.02-4 μm size range) and
87 air-exchange rate (in the range of about 0.5 -1.5 h⁻¹) measurements carried out in nine homes with
88 sampling duration from 6 to 12 consecutive days. The F_{in} relative to the FMPS size class were
89 estimated by interpolation with a cubic spline [34] (Fig. S1 of supplemental material). For
90 aerodynamic diameters (0.01-0.02 μm) outside the Bennett and Koutrakis [33] measurement range
91 the F_{in} value of 0.02 μm particles was adopted.

92 Throughout the aerosol measurements atmospheric pressure, temperature, relative humidity,
93 wind speed and wind direction were continuously measured with 5 min averaging time (Fig. S2 of
94 supplemental material).

95

96 2.2. Aerosol dosimetry

97 To estimate aerosol doses due to the infiltration of outdoor aerosol in indoor environments, 22
 98 hours daily indoor residence was supposed. Three time periods (t_r) were assumed according to the
 99 different work physical activities: 7 hours sleeping (from 11pm to 6 am), three hours sitting awake (6-7
 100 am and 9-11 pm), 12 hours light work (8am-4 pm and 5pm-9pm). The particle regional deposition
 101 fractions per ($F^R(d_{ai})$) as a function of aerodynamic diameter (d_{ai}) have been estimated using the Multiple-
 102 Path Particle model Dosimetry (MPPD v3.01, ARA 2015, ARA, Arlington, VA, USA) [33]. The 60th
 103 percentile human stochastic lung was considered along with the following settings: (i) a uniformly
 104 expanding flow, (ii) an upright body orientation, and (iii) nasal breathing with a 0.5 inspiratory fraction
 105 and no pause fraction. Moreover, the following parameters were used for a Caucasian adult male under
 106 light work physical activity, based on the ICRP report [36]: (i) a functional residual capacity (FRC) of
 107 3300 mL, (ii) an upper respiratory tract (URT) volume equal to 50 mL, (iii) a breathing frequency of 12
 108 min^{-1} for sleeping and sitting awake activity and 20 min^{-1} for light work activity, and (iv) an air volume
 109 inhaled during a single breath (tidal volume, V_t) of 0.625 L, 0.750L and 1.25 L, respectively for sleeping,
 110 sitting awake and light work activities.

111 Since FMPS measures aerosol size number distribution as a function of the electrical mobility
 112 diameter (d), d values have been transformed to aerodynamic diameter (d_a) according to equation (1)
 113 [37].

$$d_a = d \sqrt{\chi \times \frac{\rho \times C_c(d_m)}{C_c(d_a)}}, \quad (1)$$

114 where C_c is the Cunningham slip factor for a given diameter, ρ is the particle density (1.5 g cm^{-3} density
 115 was assumed) and χ is the particle dynamic shape factor. χ as a function of aerodynamic diameter was
 116 estimated by interpolating with a cubic spline the data reported by Hu et al. [38] in the range from 0.1
 117 to 1.8 μm in Beijing. For d_a outside below this range the relevant lower bound χ value was adopted
 118 (1.13 for $d_a < 0.1 \mu\text{m}$).

119 Aerosol number doses $D^R(d_{ai}, t)$ deposited in the head (H), tracheobronchial (TB) and alveolar (Al)
 120 regions, as functions of time (t) and of the aerodynamic diameter (d_{ai}) were estimated according to eq.
 121 2:

$$D^R(d_{ai}, t) = F_{in} \times C(d_{ai}, t) \times F^R(d_{ai}) \times V_t \quad R=H, TB, Al, \quad (2)$$

122 where $C(d_{ai}, t)$ is the average aerosol concentration over a single inspiratory act as a function of time and
 123 of aerodynamic diameter.

124 Total regional aerosol doses have been estimated according to eq. 3, where the summation is
 125 carried out over the FMPS size classes:

$$D_{Tot}^R(t) = \sum_i D^R(d_{ai}, t) \quad R=H, TB, Al, \quad (3)$$

126 Total aerosol doses deposited into the respiratory system has been calculated according to eq. 4:

$$D_{Tot}^{Tot}(t) = D_{Tot}^H(t) + D_{Tot}^{TB}(t) + D_{Tot}^{Al}(t), \quad (4)$$

127 Cumulative regional and total doses over a given residence time (t_r) have been calculated
 128 according equations 5 and 6:

$$D_{Tot}^R(t_r) = \sum_{t=0}^{t_r} D_{Tot}^R(t) \quad R=H, TB, Al, \quad (5)$$

$$D_{Tot}^{Tot}(t_r) = \sum_{t=0}^{t_r} D_{Tot}^{Tot}(t), \quad (6)$$

129 The cumulative regional ($D_{Tot}^R(t_{day})$) and total daily dose ($D_{Tot}^{Tot}(t_{day})$) has been calculated as the
 130 sum of the $D_{Tot}^R(t_r)$ and $D_{Tot}^{Tot}(t_r)$ doses relative to the tree time period (t_r) considered (7 h sleeping, 3
 131 h sitting awake, 12 h light work, $t_{day}=22$ h).

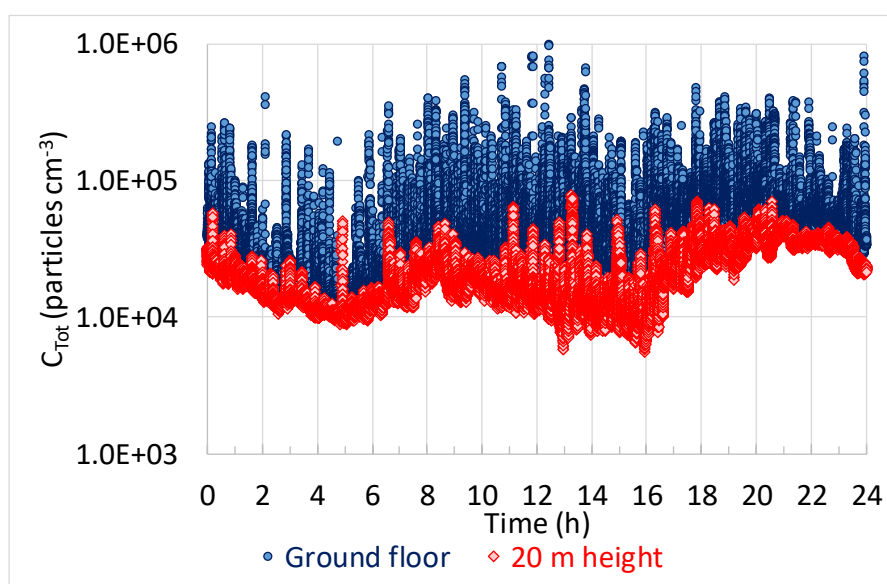
132 The cumulative total dose size distribution over a given residence time ($D^{Tot}(d_{ai}, t_r)$) has been
 133 calculated according to eq. 7:

$$D^{Tot}(d_{ai}, t_r) = \sum_{t=0}^{t_r} D^H(d_{ai}, t) + D^{TB}(d_{ai}, t) + D^{Al}(d_{ai}, t), \quad (7)$$

134

135 **3. Results and discussion**136 *3.1. Aerosol measurements*

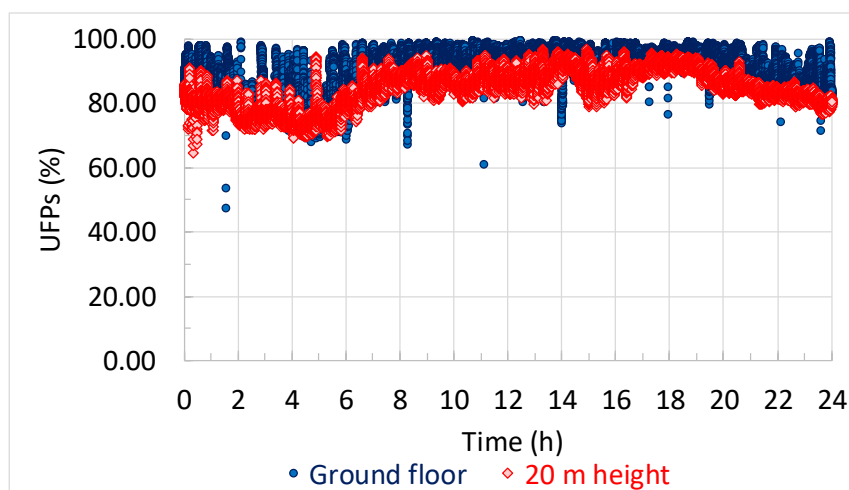
137 Outdoor aerosol total number concentrations (C_{Tot}) over the 24 hours considered were on
 138 average 2.3-fold higher at ground floor than at 20 m heights with spike concentration ratios exceeding
 139 20, up to about 40. Both sets of data shared the same temporal modulation with two broad peaks
 140 centered at 8 am and 7 pm, determined by the daily traffic flow variation and by the planetary
 141 boundary layer (PBL) mixing height that was highest in the central part of the day during period of
 142 high solar radiation (Figure 1) [39-41].



143

144 **Figure 1.** Total (5.6-560 nm electrical mobility diameter) aerosol concentrations measured with 1 s time
 145 resolution at ground floor and at 20 m height in a street canyon in downtown Rome.

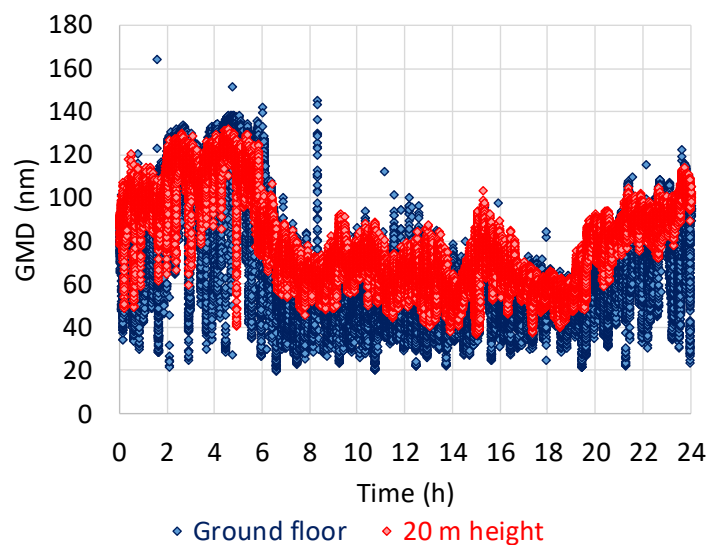
146 Spike concentration were more intense and frequent at ground level than at 20 m heights due to
 147 the proximity of the vehicular exhausts. The contribution of UFPs at ground level was slightly higher
 148 than at 20 m height, on average respectively 88% and 84%, although at ground level it occasionally
 149 dropped below the relevant value at 20 m height. Such occurrence was probably due to the turbulence
 150 at ground level generated by the vehicular traffic, with consequent dust re-suspension and removal
 151 of smaller particles by impaction.



152

153 **Figure 2.** Temporal trend of UFP % contribution at ground floor and at 20 m height in a street canyon in
154 downtown Rome.

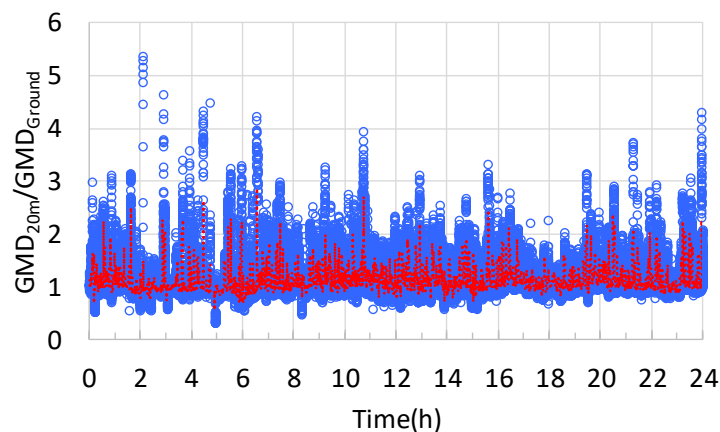
155 Small particles ($< 0.1 \mu\text{m}$) deposition is efficient due to their Brownian diffusion, whereas
156 interception, impaction and gravitational settling are important deposition mechanism for larger
157 particles ($> 2 \mu\text{m}$) [42]. Minimum values of deposition velocities occur for particles in the range 0.1-2
158 μm , because neither Brownian diffusion nor impaction or interception are effective mechanisms [42].
159 Consequently, nucleation particles are less persistent than larger-sized particles. Therefore, they are
160 predominant during traffic hours, when freshly formed from vehicular exhausts and decrease
161 significantly at night, when traffic is less intense and particles in the accumulation mode predominate.
162 Therefore, Geometric Mean Diameter (GMD), both at ground level and at 20 m height (Figure 3),
163 follows a temporal trend a characterized by low values during the day and increases during nocturnal
164 hours.



165

166 **Figure 3.** Temporal trend of the Geometric Mean aerodynamic Diameter (GMD) at ground level and at 20
167 m height in a street canyon in downtown Rome.

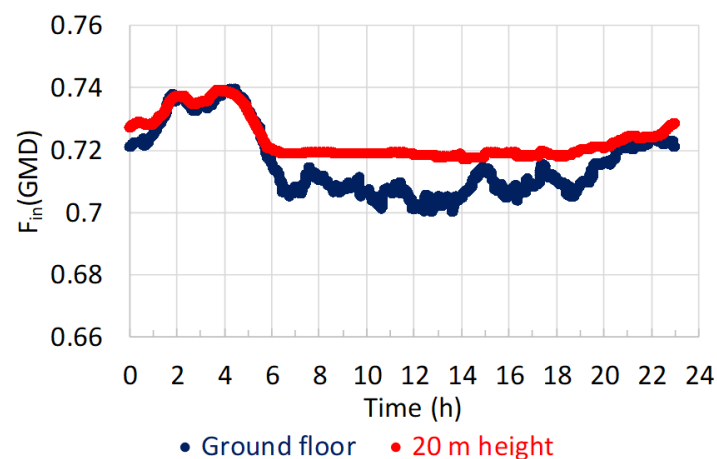
168 For these reasons, and due to the higher distance from the traffic exhaust, as a general trend
169 GMD is higher at 20 m height than at ground level, as shown in Figure 4, where the ratio of GMD at
170 the two levels is plotted as a function of time. This feature involves some consequences in terms of
171 aerosol capability of infiltrating indoor environments.



172

173 **Figure 4.** Ratio of geometric mean aerodynamic diameter (GMD) at 20 m height to GMD at ground level in
174 a street canyon in downtown Rome.

175 To discuss this point, the infiltration factors pertaining to each GMD value have been calculated
176 at both levels (Figure 5). Such dataset, being characterized by highly frequent spike values, has been
177 despiked by calculating the relevant 1h mobile averages ($F_{in}(GMD)$). The smoothed dataset so
178 obtained allows to assess a general daily trend of the average infiltration factor (Figure 5). At both
179 levels the $F_{in}(GMD)$ is higher during nocturnal hours than during daytime, in the same periods when
180 a maximum is observed in the GMD temporal trends (Figure 3). Moreover, due to the higher GMD
181 values, the aerosol infiltration efficiency at 20 m height is, on average, slightly higher than at ground
182 level.



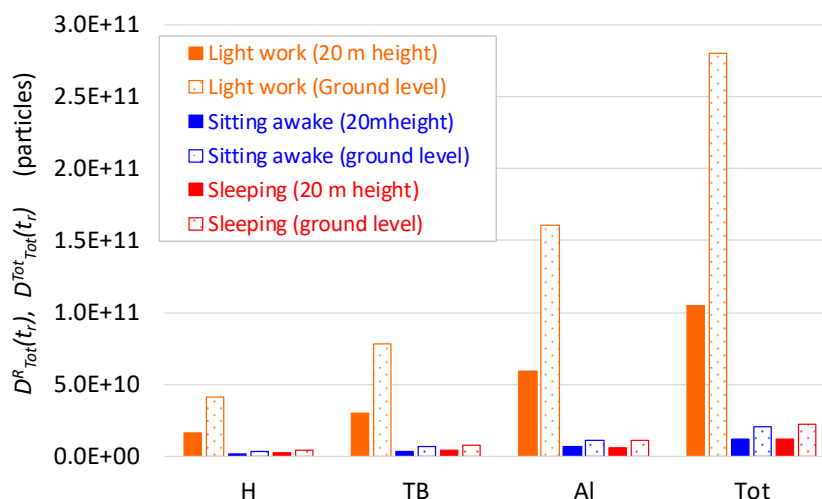
183

184 **Figure 5.** 1h-moving average of the infiltration factors (F_{in}) calculated at the GMD values at ground level
185 and at 20 m height.

186 This occurs because the infiltration efficiency for small particles ($< 0.1 \mu\text{m}$) due to their efficient
187 Brownian deposition is lower than for accumulation mode particles.

188 3.2. Aerosol dosimetry

189 Figure 6 describes the cumulative regional ($D_{Tot}^R(t_r)$) and total dose ($D_{Tot}^{Tot}(t_r)$) estimated for
190 indoor environments at ground floor and at 20 m height, in the absence of indoor aerosol emission
191 sources. They represent the contribution due to the indoor infiltration of outdoor aerosol. These doses
192 are about 2.6, 1.7 and 1.9-fold higher at ground floor than at 20 m height, respectively for light work,
193 sitting awake and sleeping physical activities. Such differences are determined by the higher outdoor
194 aerosol concentrations at the street level (Figure 1) that abundantly outweigh the higher average
195 infiltration efficiency of the aerosol at 20 m height (Figure 5). The highest $D_{Tot}^{Tot}(t_r)$ doses have been
196 estimated during the period of light work activity (1.05×10^{11} particles at 20 m height and 2.80×10^{11}
197 particles at ground floor) and the lowest for sitting awake activity (1.20×10^{10} particles at 20 m height
198 and 2.02×10^{10} particles at ground floor) because of both the longer time period and of the higher tidal
199 volume and breathing frequency for light work activities.

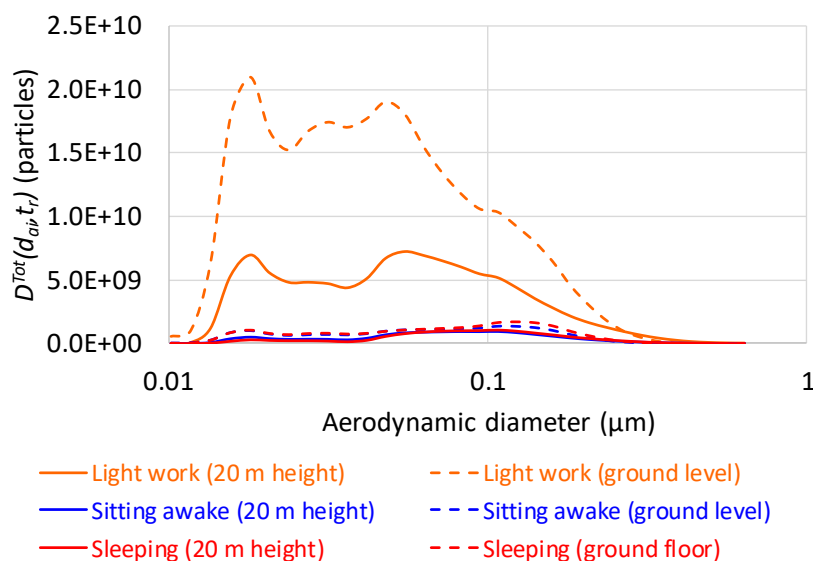


200

201 **Figure 6.** Cumulative regional ($D_{Tot}^R(t_r)$) and total ($D_{Tot}^{Tot}(t_r)$) aerosol doses over a residence time (t_r) of 7 h,
 202 3 h and 12 h, respectively for sleeping, sitting awake and light work activities, at ground level and at 20 m
 203 height.

204 The different work activities also affect the particle dose distribution within the respiratory
 205 system. The fraction of particles deposited in the H and TB regions decreases passing from sleeping
 206 (respectively 17% and 33%) to light work activity (respectively 15% and 28%); conversely, the AI
 207 fraction increases (from 50% to 57%).

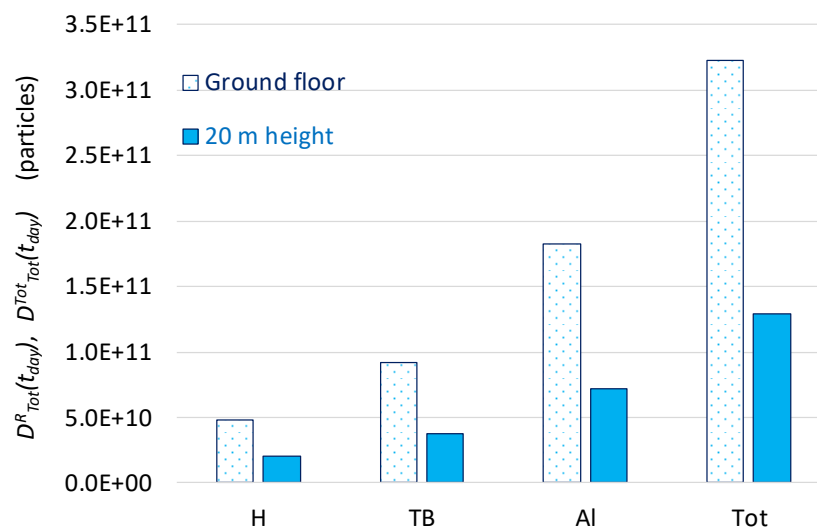
208 Figure 7 shows the size distributions of $D_{Tot}^R(t_r)$ doses at ground level and at 20 m height. For
 209 light work activity, at both levels, three modes of about the same importance were present at 0.018,
 210 0.031 and 0.048 μm and a fourth one, less intense, at about 0.107 μm . The first two modes occurred
 211 also for the sitting awake and sleeping activities, but the more intense modes were at higher particle
 212 diameters (0.072 and 0.120 μm), reflecting the more abundant presence of accumulation mode
 213 particles during nocturnal hours.



214

215 **Figure 7.** Cumulative total dose size distribution ($D_{Tot}^{Tot}(d_{ai}, t_r)$) at ground level and at 20 m height, over a
 216 residence time (t_r) of 7 h, 3 h and 12 h, respectively for sleeping, sitting awake and light work activities.

217 Figure 8 describes the cumulative regional ($D_{Tot}^R(t_{day})$) and total ($D_{Tot}^{Tot}(t_{day})$) daily doses
 218 estimated for one day residence in an indoor environment at ground floor and at 20 m height. 3.23×10^{11}
 219 and 1.29×10^{11} particles are respectively deposited into the respiratory system at ground floor and at 20
 220 m height. About 16 %, 29 % and 55 % of such doses are respectively deposited in the H, TB and Al
 221 regions.

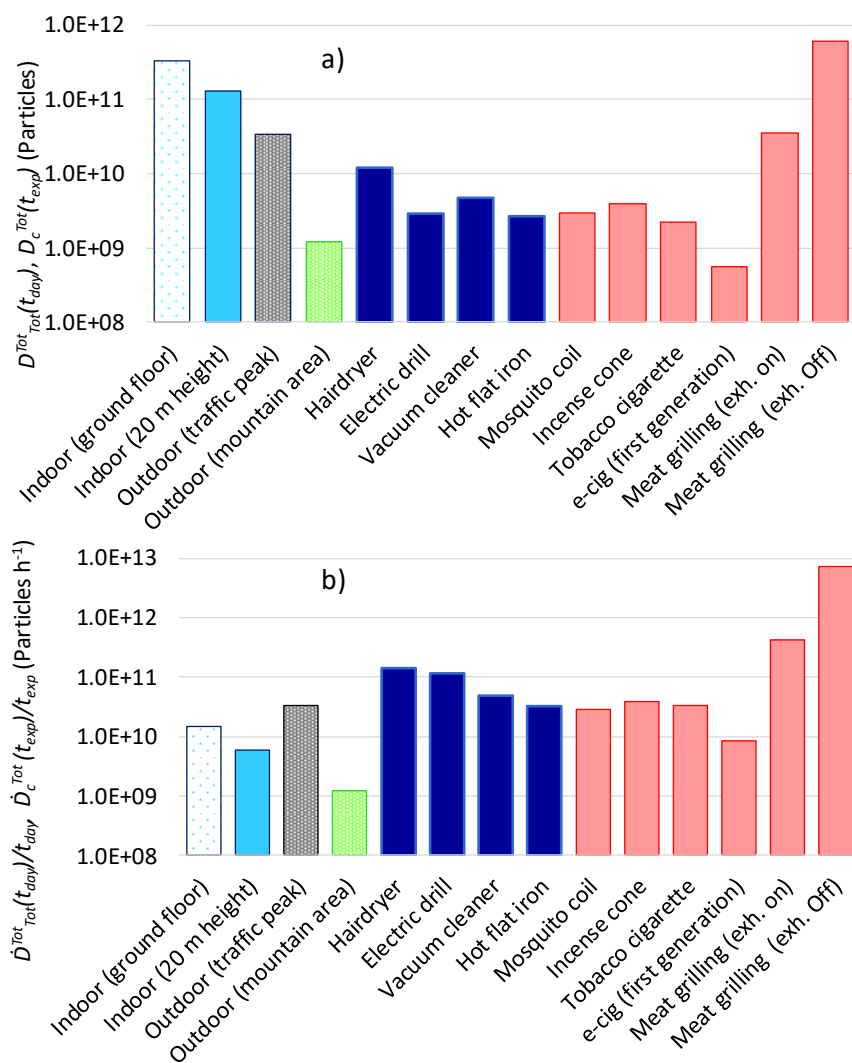


222

223 **Figure 8.** Cumulative regional ($D_{Tot}^R(t_{day})$) and total daily dose ($D_{Tot}^{Tot}(t_{day})$) at ground level and at 20 m
 224 height.

225 $D_{Tot}^{Tot}(t_{day})$ at both levels are compared in Figure 9a with the total particle doses deposited into
 226 the respiratory system after 1 h exposure time (t_{exp}), at the same site and in the same day, at outdoor
 227 aerosol during the traffic peak hour and after 1h exposure to atmospheric aerosol in Mount
 228 Terminillo, a central Italy 2217 m high mount region ($D_c^{Tot}(t_{exp})$) [43]. In the same figure the
 229 comparison is carried out with the main combustion and non-combustion sources encountered in
 230 indoor environments [21-24], in this case t_{exp} represents the period of source operation (5, 1.5, 6, 5, 6,
 231 6, 4, 4 and 5 min) respectively for hairdryer, electric drill, vacuum cleaner, hot flat iron, mosquito coil,
 232 incense cone, tobacco cigarette, e-cigarette and meat grilling.

233 Due to the longer exposure time (22 h), at both levels $D_{Tot}^{Tot}(t_{day})$ are higher than the doses relative
 234 to all the other operations, with the exception of the meat grilling without exhaust ventilation. In that
 235 case, a single 5 min exposure is associated to a dose that is 1.9 and 4.7 fold higher than the cumulative
 236 total daily doses at ground floor and 20 m height (22 h exposure). To account for the different time
 237 scales, the doses of Figure 9a have been referred to unit exposure time ($\dot{D}_{Tot}^{Tot}(t_{day})$, $\dot{D}_c^{Tot}(t_{exp})$) and
 238 plotted in Figure 9b. On this basis, with the exception of the relatively low aerosol emitting first
 239 generation e-cigarette [21,23], all the doses due to indoor aerosol sources are higher than the doses due
 240 to the infiltration of outdoor particles.



241

242 **Figure 9.** (a) $D_{Tot}^{Tot}(t_{day})$ at ground level and at 20 m height compared with the total particle doses deposited
 243 into the respiratory system ($D_c^{Tot}(t_{exp})$) after exposure to different indoor and outdoor aerosol sources for
 244 given exposure times (t_{exp}); (b) The same comparison is made for the relevant doses per unit exposure time
 245 ($\dot{D}_{Tot}^{Tot}(t_{day}), \dot{D}_c^{Tot}(t_{exp})$).

246 Moreover, the dose after 1h outdoor exposure in the Terminillo mountain area emphasizes the
 247 influence of the outdoor pollution on indoor air quality. Such dose is 12 and 5-fold lower than the 1
 248 h doses relative respectively to the ground floor and to the 20 m height indoor environments in an
 249 urban street canyon.

250

251 4. Conclusions

252 Particle number size distributions have been simultaneously measured at street level and at
 253 about 20 m height, with 1 s time resolution, at a street canyon in downtown Rome. At both heights,
 254 the total particle number concentrations shared a temporal trend that on hourly time scale was
 255 determined by the daily traffic flow variations and by the PBL modulation. On a few second time
 256 scale, the two trends were characterized by spike concentrations, due to freshly emitted vehicular
 257 exhausts. Due to the closer proximity to traffic, such spikes were more frequent and more intense at
 258 ground level than at 20 m heights. This circumstance made the road level aerosol concentrations on
 259 average richer in UFPs, particularly in nucleation mode particles. Hence, the aerosol infiltration
 260 efficiency was on average slightly higher at 20 m heights than at ground level. On the other hand, for

261 the same reason, the road level aerosol concentration was on average more than double than at 20 m
262 heights. As a result of that, the indoor aerosol concentration due to the penetration of outdoor
263 particles was higher at ground floor than at 20 m height. With an estimated daily indoor permanence
264 of 22 hours, the daily dose deposited into the respiratory system was 3.23×10^{11} and 1.29×10^{11} particles
265 respectively at ground level and at 20 m height. Such doses are greater than those estimated over the
266 period of activity of some common combustion and non-combustion sources in indoor environment,
267 therefore they represent an important contribution to the total aerosol daily dose.
268

269 **Supplementary Materials:** The following are available online, Figure S1: Infiltration factors (F_{in}) estimated by
270 interpolation of the average F_{in} measured by Bennett and Koutrakis [32], Figure S2: Atmospheric pressure,
271 Temperature, Relative humidity, wind speed and wind direction throughout the aerosol measurements
272 (averaging time 5 min).

273 **Author Contributions:** conceptualization, M.M. and P.A.; methodology, M.M. and P.A.; software, M.M.;
274 validation, M.M., C.P., M.V. and P.A.; formal analysis, M.M.; writing—original draft preparation, M.M. and C.P.;
275 writing—review and editing, M.V. and P.A.

276 **Funding:** This research received no external funding.

277 **Acknowledgments:** The authors wish to thank ARA for MPPD Version 3.01. This study was carried out within
278 the context of the Research Program 2019-2021 of National Institute for Insurance against Accidents at Work
279 (INAIL).

280 **Conflicts of Interest:** The authors declare no conflict of interest.

281 References

- 282 1. World Health Organization (WHO). Air pollution. Available online: <https://www.who.int/airpollution/en/>
283 (accessed on 18 September 2019).
- 284 2. Anderson, J.O., Thundiyil, J.G., Stolbach, A. Clearing the air: a review of the effects of particulate matter
285 air pollution on human health. *J. Med. Toxicol.* **2012**, *8*, 166–175. doi: 10.1007/s13181-011-0203-1.
- 286 3. Noh, J., Sohn, J., Cho, J., Kim, C., Shin, D.C. YIA 02-02 long-term effects of fine particulate matter exposures
287 on major adverse cardiovascular events. *J. Hypertens.* **2016**, *34*, e202. doi:
288 10.1097/01.hjh.0000500437.46224.7e.
- 289 4. Wang, Y., Xiong, L., Tang, M. Toxicity of inhaled particulate matter on the central nervous system:
290 neuroinflammation, neuropsychological effects and neurodegenerative disease. *J. Appl. Toxicol.* **2017**, *37*,
291 644–667. doi: 10.1002/jat.3451.
- 292 5. International Agency for Research on Cancer (IARC). Monographs on the Evaluation of Carcinogenic Risks
293 to Humans. International Agency for Research on Cancer. Outdoor Air Pollution Volume 109. WHO Press,
294 Lyon, France, 2015. Available online: <http://monographs.iarc.fr/ENG/Monographs/vol109/index.php>
295 (accessed on 10 September 2019).
- 296 6. Brauer, M., Koutrakis, P., Spengler, J.D. Personal exposures to acidic aerosols and gases. *Environ. Sci.*
297 *Technol.* **1989**, *23*, 1408–1412. doi: 10.1021/es00069a013.
- 298 7. Avino, P., Casciardi, S., Fanizza, C., Manigrasso, M. Deep investigation of Ultrafine particles in urban air.
299 *Aerosol Air Qual. Res.* **2011**, *11*, 654–663. doi: 10.4209/aaqr.2010.10.0086.
- 300 8. Stabile, L., Buonanno, G., Avino, P., Fuoco, F.C. Dimensional and chemical characterization of airborne
301 particles in schools: Respiratory effects in children. *Aerosol Air Qual. Res.* **2013**, *13*, 887–900. doi:
302 10.4209/aaqr.2012.12.0339.
- 303 9. Pagano, P., De Zaiacom, T., Scarcella, E., Bruni, S., Calamosca, M. Mutagenic activity of total and particle-
304 sized fractions of urban particulate matter. *Environ. Sci. Technol.* **1996**, *30*, 3512–3516. doi: 10.1021/es960182q.
- 305 10. Li, N., Sioutas, C., Cho, A., Schmitz, D., Misra, C., Sempf, J., Wang, M., Oberley, T., Froines, J., Nel, A.
306 Ultrafine particulate pollutants induce oxidative stress and mitochondrial damage. *Environ. Health Perspect.*
307 **2003**, *11*, 455–460. doi: 10.1289/ehp.6000.
- 308 11. Chen, R., Hu, B., Liu, Y., Xu, J., Yang, G., Xu, D., Chen, C. Beyond PM_{2.5}: The role of ultrafine particles on
309 adverse health effects of air pollution. *Biochim. Biophys. Acta.* **2016**, *1860*, 2844–2855. doi:
310 10.1016/j.bbagen.2016.03.019.

- 311 12. Calderón-Garcidueñas, L., Calderón-Garcidueñas, A., Torres-Jardón, R., Avila-Ramírez, J., Kulesza, R.J.,
312 Angiulli, A.D. Air pollution and your brain: what do you need to know right now. *Prim. Health Care Res.*
313 *Dev.* **2015**, *16*, 329-345. doi: 10.1017/S146342361400036X.
- 314 13. da Costa, E., Oliveira, J.R., Base, L.H., de Abreu, L.C., Filho, C.F., Ferreira, C., Morawska, L. Ultrafine
315 particles and children's health: Literature review. *Paediatr. Respir. Rev.* (in press). doi:
316 10.1016/j.prrv.2019.06.003.
- 317 14. Manigrasso, M., Protano, C., Vitali, M., Avino, P. Where do Ultrafine Particles and Nano-Sized Particles
318 come from? *J. Alzheimers Dis.* **2019**, *68*, 1371-1390. doi: 10.3233/JAD-181266.
- 319 15. Avino, P., Protano, C., Vitali, M., Manigrasso, M. Benchmark study on fine-mode aerosol in a big urban
320 area and relevant doses deposited in the human respiratory tract. *Environ. Pollut.* **2016**, *216*, 530-537. doi:
321 10.1016/j.envpol.2016.06.005.
- 322 16. Manigrasso, M., Avino, P. Fast evolution of urban ultrafine particles: Implications for deposition doses.
323 *Atmos Environ.* **2012**, *51*, 116-123. doi: 10.1016/j.atmosenv.2012.01.039.
- 324 17. Manigrasso, M., Vernale, C., Avino, P. Traffic aerosol lobar doses deposited in the human respiratory
325 system. *Environ. Sci. Pollut. Res. Int.* **2017**, *24*, 13866-13873. doi: 10.1007/s11356-015-5666-1.
- 326 18. Manigrasso, M., Natale, C., Vitali, M., Protano, C., Avino, P. Pedestrians in traffic environments: ultrafine
327 particle respiratory doses. *Int. J. Environ. Res. Public Health.* **2017**, *14*, pii: E288. doi: 10.3390/ijerph14030288.
- 328 19. Manigrasso, M., Buonanno, G., Stabile, L., Morawska, L., Avino, P. Particle doses in the pulmonary lobes
329 of electronic and conventional cigarette users. *Environ. Pollut.* **2015**, *202*, 24-31. doi:
330 10.1016/j.envpol.2015.03.008.
- 331 20. Manigrasso, M., Vitali, M., Protano, C., Avino, P. Temporal evolution of ultrafine particles and of alveolar
332 deposited surface area from main indoor combustion and non-combustion sources in a model room. *Sci.*
333 *Total Environ.* **2017**, *598*, 1015-1026. doi: 10.1016/j.scitotenv.2017.02.048.
- 334 21. Protano, C., Manigrasso, M., Avino, P., Vitali, M. Second-hand smoke generated by combustion and
335 electronic smoking devices used in real scenarios: Ultrafine particle pollution and age-related dose
336 assessment. *Environ. Int.* **2017**, *107*, 190-195. doi: 10.1016/j.envint.2017.07.014.
- 337 22. Manigrasso, M., Vitali, M., Protano, C., Avino, P. Ultrafine particles in domestic environments: Regional
338 doses deposited in the human respiratory system. *Environ. Int.* **2018**, *118*, 134-145. doi:
339 10.1016/j.envint.2018.05.049.
- 340 23. Protano, C., Avino, P., Manigrasso, M., Vivaldi, V., Perna, F., Valeriani, F., Vitali, M. Environmental
341 Electronic Vape exposure from four different generations of electronic cigarettes: airborne Particulate
342 Matter levels. *Int. J. Environ. Res. Public Health.* **2018**, *15*, E2172. doi: 10.3390/ijerph15102172.
- 343 24. Manigrasso, M., Protano, C., Astolfi, M.L., Massimi, L., Avino, P., Vitali, M., Canepari, S. Evidences of
344 copper nanoparticle exposure in indoor environments: Long-term assessment, high-resolution field
345 emission scanning electron microscopy evaluation, in silico respiratory dosimetry study and possible
346 health implications. *Sci. Total Environ.* **2019**, *653*, 1192-1203. doi: 10.1016/j.scitotenv.2018.11.044.
- 347 25. Hubal, E.A.C., Sheldon, L.S., Burke, J.M., McCurdy, T.R., Berry, M.R., Rigas, M.L., Zartarian, V.G.,
348 Freeman, N.C. Children's exposure assessment: a review of factors influencing children's exposure, and
349 the data available to characterize and assess that exposure. *Environ. Health Perspect.* **2000**, *108*, 475-486. doi:
350 10.1289/ehp.108-1638158.
- 351 26. Morawska, L., Ayoko, G.A., Bae, G.N., Buonanno, G., Chao, C.Y.H., Clifford, S., Fu, S.C., Hänninen, O., He,
352 C., Isaxon, C., Mazaheri, M., Salthammer, T., Waring, M.S., Wierzbicka, A. Airborne particles in indoor
353 environment of homes, schools, offices and aged care facilities: the main routes of exposure. *Environ. Int.*
354 **2017**, *108*, 75-83. doi: 10.1016/j.envint.2017.07.025.
- 355 27. Śmiełowska, M., Marć, M., Zabiegała, B. Indoor air quality in public utility environments-a review. *Environ.*
356 *Sci. Pollut. Res.* **2017**, *24*, 11166-11176. doi: 10.1007/s11356-017-8567-7.
- 357 28. Quang, T.N., He C., Morawska L., Knibbs L.D., Falk M. Vertical particle concentration profiles around
358 urban office buildings. *Atmos. Chem. Phys.* **2012**, *12*, 5017-5030. doi: 10.5194/acp-12-5017-2012.
- 359 29. Goel A., Kumar P. Vertical and horizontal variability in airborne nanoparticles and their exposure around
360 signalised traffic intersections. *Environ. Pollut.* **2016**, *214*, 54-69. doi: 10.1016/j.envpol.2016.03.033.
- 361 30. Kuuluvainen, H., Poikkimäki, M., Järvinen, A., Kuula, J., Irjala, M., Dal Maso, M., Keskinen, J., Timonen,
362 H., Niemi, J.V., Rönkkö T. Vertical profiles of lung deposited surface area concentration of particulate
363 matter measured with a drone in a street canyon. *Environ. Pollut.* **2018**, *241*, 96-105. doi:
364 10.1016/j.envpol.2018.04.100.

- 365 31. TSI Particle technology, 2009. Available online:
366 www.tsi.com/uploadedFiles/Product_Information/Literature/Catalogs/Particle_Catalog_Web.pdf
367 (accessed on 10 September 2019).
- 368 32. Jeong, C.-H., Greg, J., Evans, G.J. Inter-comparison of a fast mobility particle sizer and a scanning mobility
369 particle sizer incorporating an ultrafine water based condensation particle counter. *Aerosol Sci. Technol.* **2009**,
370 *43*, 364-373. doi: 10.1080/02786820802662939.
- 371 33. Bennett, D.H., Koutrakis, P. Determining the infiltration of outdoor particles in the indoor environment
372 using a dynamic model. *Aerosol Sci.* **2006**, *37*, 766-785. doi: 10.1016/j.jaerosci.2005.05.020.
- 373 34. De Boor, C. A Practical Guide to Splines. Springer-Verlag: New York, 1978.
- 374 35. Asgharian, B., Hofmann, W., Bergmann, R. Particle deposition in a multiple-path model of the human lung.
375 *Aerosol Sci. Technol.* **2001**, *34*, 332-339. doi: 10.1080/02786820151092478.
- 376 36. International Commission on Radiological Protection (ICRP). Publication 66: Human Respiratory Tract Model
377 for Radiological Protection. Elsevier Science: Oxford, U.K., 1994.
- 378 37. Li, X., Yan, C., Patterson, R.F., Zhu, Y., Yao, X., Zhu, Y., Ma, S., Qiu, X., Zhu, T., Zheng, M. Modeled
379 deposition of fine particles in human airway in Beijing, China. *Atmos. Environ.* **2016**, *124*, 387-395. doi:
380 10.1016/j.atmosenv.2015.06.045.
- 381 38. Hu, M., Peng, J., Sun, K., Yue, D., Guo, S., Wiedensohler, A., Wu, Z. Estimation of size-resolved ambient
382 particle density based on the measurement of aerosol number, mass, and chemical size distributions in the
383 winter in Beijing. *Environ. Sci. Technol.* **2012**, *46*, 9941-9947. doi: 10.1021/es204073t.
- 384 39. Avino, P., Brocco, D., Lepore, L., Pareti, S. Interpretation of atmospheric pollution phenomena in
385 relationship with the vertical atmospheric remixing by means of natural radioactivity measurements
386 (radon) of particulate matter. *Ann. Chim-Rome.* **2003**, *93*, 589-594.
- 387 40. Avino, P., Manigrasso, M. Dynamic of submicrometer particles in urban environment. *Environ. Sci. Pollut.*
388 *Res. Int.* **2017**, *24*, 13908-13920. doi: 10.1007/s11356-016-6752-8.
- 389 41. Manigrasso, M., Febo, A., Guglielmi, F., Ciambottini, V., Avino, P. Relevance of aerosol size spectrum
390 analysis as support to qualitative source apportionment studies. *Environ. Pollut.* **2012**, *170*, 43-51. doi:
391 10.1016/j.envpol.2012.06.002.
- 392 42. Zhang, L., Gong, S., Padro, J., Barrie, L. A size-segregated particle dry deposition scheme for an
393 atmospheric aerosol module. *Atm. Environ.* **2001**, *35*, 549-560. doi: 10.1016/S1352-2310(00)00326-5.
- 394 43. Manigrasso, M., Protano, C., Martellucci, S., Mattei, V., Vitali, M., Avino, P. Evaluation of the Submicron
395 Particles distribution between mountain and urban site: contribution of the transportation for defining
396 environmental and human health issues. *Int. J. Environ. Res. Public Health* **2019**, *16*, 1339. doi:
397 10.3390/ijerph16081339.